ELSEVIER

Journal of Alloys and Compounds 424 (2006) 78–87

Journal of ALLOYS AND COMPOUNDS

www.elsevier.com/locate/jallcom

Comparative analysis of the chlorination of mixtures iron–aluminum and the binary alloy $FeAl_3$

Fabiola J. Alvarez [a,*], Daniel M. Pasquevich [a,b], Ana E. Bohé [b,c]

[a] *Comisión Nacional de Energía Atómica, Centro Atómico Bariloche, Av. Bustillo 9500, (8400) San Carlos de Bariloche, Rio Negro, Argentina*
[b] *Consejo Nacional de Investigaciones Científicas y Técnicas, Argentina*
[c] *Centro Regional Universitario Bariloche, Universidad Nacional del Comahue, Argentina*

Received 21 October 2005; received in revised form 19 December 2005; accepted 20 December 2005
Available online 7 February 2006

Abstract

A comparative study of the behavior of a binary alloy $FeAl_3$ and an equivalent mixture of the pure metals towards chlorine, was carried out between 150 and 300 °C. The present work focuses at the analysis of the interactions between metals and the possibility of their separation. According to the composition determined for the $AlCl_3$ obtained from the reactants, the separation of the metals was more effective in the case of the alloy, while for the $FeCl_3$ the segregation of the aluminum from the iron was better in the mixture than in the alloy. The last result could be revealing a stronger interaction between the chlorides in the alloy.

The reactants, products and residues were identified, characterized and quantified by X-ray diffraction (XRD), scanning electron microscopy (SEM), Mössbauer spectroscopy (MS), chemical analysis (atomic absorption, spectrophotometry and gravimetry) and X-ray fluorescence spectrometry (XRF).

Keywords: Gas–solid reactions; Chemical synthesis; Corrosion; X-ray diffraction; Scanning electron microscopy

1. Introduction

Aluminum chloride has a monoclinic crystal structure with the lattice dimensions: $a = 5.914$, $b = 10.234$, $c = 6.148$ and $\beta = 108.3$ [1]. It crystallizes in pseudohexagonal habit (twinned). When pure, is a white solid; however, the commercial product is marketed in a range of colors: orange, yellow, gray and greenish. Besides, depending upon its method of collection during manufacture, it may be either a powder or a crystalline material of various mesh sizes [2]. The chloride fumes in moist air, owing to the formation of hydrochloric acid and $AlCl_3{\cdot}6H_2O$, of the rhombohedral crystalline system, which is yellowish-white to colorless.

In the presence of an excess of chlorine, iron forms ferric chloride [3], with the characteristic dark-green highly hygroscopic hexagonal crystals, and on exposure to air form a series of hydrates; with 2, 5, 6 water molecules [4].

Oersted first prepared anhydrous aluminum chloride in 1825 by the reaction of chlorine gas with a mixture of alumina and carbon [5]. Most anhydrous aluminum chloride is made by chlorinating the metal, chlorine is passed through molten aluminum in a tube-shaped reactor, while the temperature is maintained at 670–850 °C by controlling the admission rates of chlorine and aluminum and by cooling the reactor walls with water. The aluminum chloride vapor leaving the reactor is passed through ceramic-lined tubes into large, air-cooled iron chambers. Solid aluminum chloride is withdrawn from the condenser walls at regular intervals, ground and classified by sieving. Chlorine in the off-gas is removed by conventional methods, such as absorption in caustic soda solution [6].

Another way of preparing the halide is the chlorination of the molten metal in a refractory crucible, sparging chlorine over the surface. As it is an exothermic reaction, the removed heat allows the volatilization of the chloride [7]. Among the most popular methods there is the reaction between aluminum powder and gaseous hydrogen chloride inside a glass tube in an electric furnace [8]. Moreover, aluminum trichloride vapors may be obtained by sparging a molten aluminum bed with primary chlorine in an enclosed zone at temperatures between

* Corresponding author.
E-mail address: alvarezf@cab.cnea.gov.ar (F.J. Alvarez).

0925-8388/$ – see front matter © 2006 Elsevier B.V. All rights reserved.
doi:10.1016/j.jallcom.2005.12.079

680 and 760 °C. Finally, the product is burnt with a mixture of hydrogen–air, and collected as finely-divided alumina [9]. Non-agglomerated anhydrous aluminum chloride is formed after the action of chlorine on a fluidized bed of aluminum particles and a powdered inert material like native rutile, in a range of temperatures between 200 and 300 °C [10].

Several works proposed different methods for the synthesis of iron(III) chloride, from the metal or the oxide, for example the direct combustion of metallic iron in dry chlorine [11], or by reaction of ferric oxide with gaseous chlorine between 700 and 1000 °C [12]. The chlorine–iron(III) chloride system has been studied in detail, determining that when $FeCl_3$ are grown from the gas phase with sufficient chlorine present to prevent the formation of $FeCl_2$, $FeCl_3$ crystals contain some $FeCl_2$ formed in solid solution. Nevertheless, the chloride content decreases with increasing chlorine pressure [13]. As it was exposed before, there are less studies about iron chlorination than that existent on aluminum reaction with chlorine, probably due to its relevance from the technology interest.

The corrosion of Fe_3Al in Cl_2–Ar mixtures has been investigated at the temperature range of 600–800 °C using thermogravimetric analysis [14]. Ko et al. separated $AlCl_3$ from $FeCl_3$ using fractional distillation, after obtaining the chlorides by chlorination of the metals at 340 °C, with mixtures Cl_2–N_2 at 100 ml/min each, for 5 h [15].

In a previous study, most favorable conditions to selectively form the volatile aluminum chloride from a HEU Al-U spent fuel were theoretically determined by thermodynamic calculations [16]. An analysis performed later demonstrates that it is technically possible to apply the background available on chlorination reactions to reprocessing of Al-U spent fuels, with some potentially valuable advantages with respect to conventional aqueous process. The thermogravimetric experiments performed during the chlorination of the cladding alloy shows this reaction is kinetically feasible at low temperatures, i.e. 473 K [17]. Another studies on thermodynamic analysis and experimental data of kinetics revealed a selective chlorination of aluminum, which volatilizes as aluminum chloride during the chlorination [18].

An oxy-chlorination process was proposed consisting of consecutive steps of chlorination followed by the oxidation of gaseous chlorides, to be applied for producing aluminum oxide in different phases depending on the p_{Cl_2} used [19]. According to some experiments done on the chlorination of AA6061, a complete volatilization of aluminum was attained at temperatures higher than 200 °C, removing low amounts of other constituents of the alloy [20]. The chlorination of AA6061 and CuZnAl alloy was carried out, revealing the complete volatilization of aluminum chloride. The chlorination started at 110 °C for AA6061 and at 300 °C for CuZnAl alloy [21]. In a more recent study the separation of several binary mixture, like Al–Fe, Al–Ni, Al–Cu, Al–Zn, etc., was performed, and the interactions between the different chlorides was determined [22].

In a previous work a theoretical and experimental study was given for the recovery of Al_2O_3 particles from a commercial aluminum-matrix composite, showing that the chlorination is feasible above 205 °C [23]. The chlorination process has also shown being an easy separation technique for complex materials, allowing the metals to turn into their respective chlorides [24].

In the present work, the separation of iron and aluminum chlorides was studied. Direct chlorination of mixtures Fe–Al 50 wt.% and of a commercial $FeAl_3$ alloy, was carried out in the temperature range 150–300 °C. The composition of the resulting chlorides was investigated by SEM, XRD, XRF and chemical analysis.

2. Experimental details

The gas used was Cl_2 99.8% purity (Indupa, Argentina). The solids were aluminum plates 99.99 wt.% (Atomergic Chemetals Corp.), iron lumps 99.98 wt.% (Aldrich) and $FeAl_3$-325 mesh powder, intermetallic, 99 wt.% metal basis (Alfa Aesar). Quantitative analysis of the starting materials was made by atomic absorption, and spectrophotometry, the composition found is the following:

- Aluminum: 99.83 wt.% Al, 0.06 wt.% Fe, 0.08 wt.% Si and 0.03 wt.% Zn.
- Iron: 99.96 wt.% Fe and 0.04 wt.% Zn.
- $FeAl_3$: 63.11 wt.% Al, 36.88 wt.% Fe and 0.01 wt.% Cu.

Direct chlorination of the reagents was performed in a reactor in chlorine flow. A raw mixture was prepared with iron and aluminum at an atomic ratio of Fe:Al = 1:2. These samples and the $FeAl_3$ alloy of about 300 mg were placed in crucibles in a tubular reactor, both made of glass, and they were placed into a horizontal electric furnace. The reactor has an "L" shape, with an elbow at the exit of the gases, surrounded by a heating winding, maintained at 200 °C. Below the end of the elbow, there is a cold vessel where the condensed substances are collected.

Another configuration used in the chlorination has a vertical furnace with book shape around the elbow, adjacent to the first reactor. This design gives an homogeneous temperature distribution along the "L" of the reactor, making easy its separation from the line.

The reactor was purged with a flow of 2 l/h chlorine for 1 h, afterwards it was heated with a ramp of 19 °C/min until it reaches the corresponding temperature of the experiment. Since then, the thermal treatments were done isothermally in chlorine atmosphere at 150, 175, 200, 225, 250, 275 and 300 °C, for periods of 1 h.

The products were removed from different temperatures zones of the reactor, while the residues remained in the crucible. Due to the hygrospicity of the products, the powders coming from the reactor were isolated into a glove box and were prepared in well sealed samplers in order to be characterized by X-ray diffraction (XRD), avoiding the absorption of moisture.

The residues were also characterized by XRD, but using samplers that did not isolate the specimen from contact with the atmosphere.

Moreover, the substances were identified by energy-dispersive spectroscopy (EDS), scanning electron microscopy (SEM) techniques and chemically quantified by atomic absorption and spectrophotometric analysis. Besides, Mössbauer spectroscopy (MS) was carried out in some samples, in order to provide information about the environment of the atom in the solid material. X-ray fluorescence spectrometry (XRF) was used to corroborate the atomic absorption results.

In order to evaluate the starting temperature for the reaction of the reagents with pure gaseous chlorine, a non-isothermic experiment was carried out, it was done in the thermogravimetric analyser based on a Cahn 2000 electrobalance, the system has been described elsewhere [25].

Samples of aluminum, iron and $FeAl_3$ between 15 and 40 mg were heated from room temperature to 276, 456 and 304 °C, for 49, 74 and 163 min, respectively. The chlorine pressure was of 36.5 kPa in flowing Ar–Cl_2 under an overall pressure of 101.3 kPa.

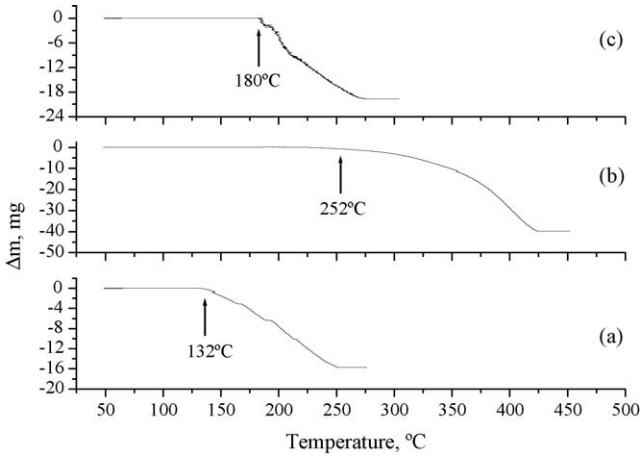

Fig. 1. Non-isothermal chlorination of 16 mg of aluminum (curve a), 40 mg of iron (curve b) and 20 mg of $FeAl_3$ (curve c). The arrow shows the starting temperature of the chlorination.

3. Results and discussion

3.1. Thermogravimetry

3.1.1. Interactions in Al–Cl_2 system

The reaction between aluminum and chlorine was studied and the results have been reported elsewhere [18]. A non-isothermal TG curve corresponding to the direct chlorination of Al is shown as curve a in Fig. 1. A progressive mass loss was detected at temperatures above 132 °C, indicating the chlorination of aluminum specimen started, and due to the high vapor pressure of $AlCl_3$ (10^{-3} kPa at 132 °C to 10^{-1} kPa at 200 °C), it vaporizes as soon as it is formed.

3.1.2. Interactions in Fe–Cl_2 system

Non-isothermal TG measurement of the chlorination of iron shown in Fig. 1b reveals mass loss at temperatures higher than 252 °C, indicating that when the iron chloride is obtained, it leaves the system as a gaseous product (if the product is $FeCl_3$, its vapor pressure will be 10^{-3} kPa at 252 °C to 10^{-1} kPa at 320 °C).

3.1.3. Interactions in Al–Fe–Cl_2 system

The reaction beginning was detected at 180 °C, followed by a rapid mass loss, owing to the vaporization of aluminum chloride firstly and secondly that of iron chloride. As seen in Fig. 1c, at 304 °C the whole sample has completely reacted with Cl_2 and has left the system with the gaseous flow.

3.2. General analysis

The reaction always occured with formation of volatile substances, and the loss of mass in the case of the binary mixtures was between 32% and 67% for the iron and of 100% for the aluminum, in the temperature range from 175 to 275 °C, while at 300 °C the reaction was completed. The product was collected in different zones of the reactor and was classified according to its temperature, while the residues and other by-products, were taken from the reaction crucible. For the alloy the loss of mass could not be determined due to the formation of by-products which remained in the reaction place, together with the residue.

Supposing the metals of the alloy form chlorides in their maximum state of oxidation, the chlorination should not leave any residue owing to their high vapor pressures. However, at low temperatures there is always some solid remaining, that diminishes as the chlorination temperature increases due to the increment in the chloride's vapor pressure.

3.3. Analysis of the reaction products

3.3.1. Mixture 50 wt.% Fe + Al

The first signs of reaction were detected at 175 °C. The products were collected from zones at different temperatures. Those deposits extracted from the lowest temperature areas presented a yellowish color and XRD analysis were performed on samples enclosed in sealed receptacles, the species identified were mainly anhydrous aluminum chlorides, $AlCl_3$ [26], whereas, at the reaction temperatures of 275 and 300 °C, $AlCl_3{\cdot}6H_2O$ [27] was also found.

A Rietveld analysis [28] was carried out to discern between the different reference patterns found for $AlCl_3$, no. 77-0819 [26] and no. 22-0010 [29]. Making use of the cell parameters cited before Ref. [1], compatibility was found with a structure that had a strong effect of preferred orientation along the (0 0 1) and (0 0 2) planes [30]. In Fig. 2 the diffractograms of the powders from different experiments, are shown. As it was said before, there is a marked orientation effect on the reflections (0 0 1) and (0 0 2), which turned out to be different than the corresponding relative intensity of the pattern. In a zone near to 2θ: 27°, there is a slight raising of the background, attributed to the growing of amorphous $AlCl_3{\cdot}6H_2O$.

From the highest temperatures areas of the reactor dark-green crystals were collected. As it is shown in Fig. 3, $FeCl_3$ [31] prevails in the product together with the hydrates (2, 5 and 6 molecules of water). The main reflections (0 0 3), (1 1 3), (1 1 6),

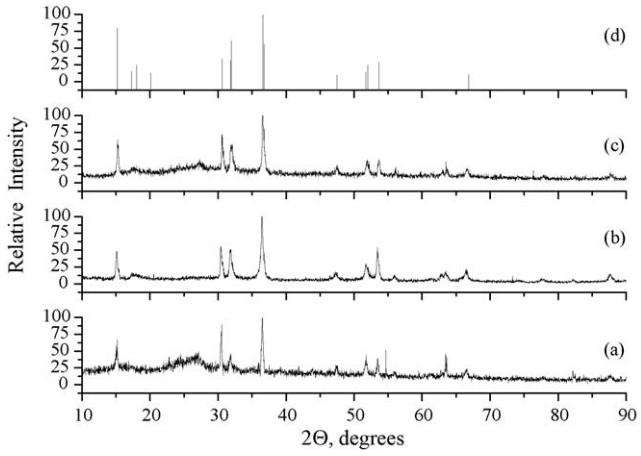

Fig. 2. Experimental diffractograms of the condensed products coming from the chlorination of the mixture Fe–50 wt.% Al and removed from the low temperature zones of the reactor: (a) product obtained at 175 °C, (b) 200 °C and (c) 300 °C. (d) Reference pattern of $AlCl_3$, card no. 77-0819.

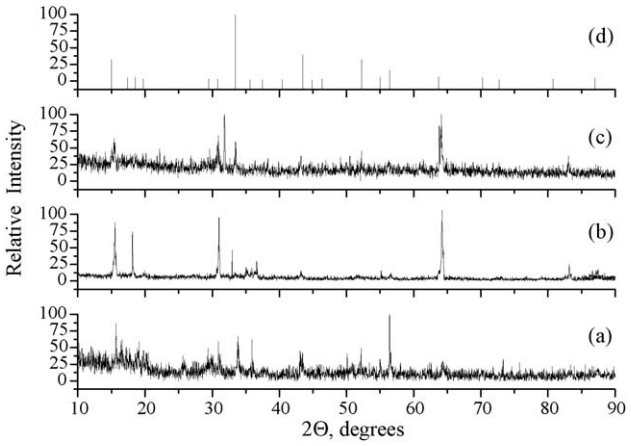

Fig. 3. Experimental diffractograms of the condensed products coming from the chlorination of the mixture Fe–50 wt.% Al and removed from the high temperature zones of the reactor: (a) product obtained at 175 °C, (b) 200 °C and (c) 250 °C. (d) Reference pattern of $FeCl_3$, card no. 1-1059.

(2 1 4) and (3 0 6) could be joint to the diffractograms for all the chlorination temperatures, exhibiting preferred orientation, with regard to the relative intensities of the ferric chloride's pattern. There is also an increment in the noise detected, due to the incipient appearance of the hydrates.

These products were simultaneously prepared into the glove box for Mössbauer analysis. It was observed a single peak with an isomeric shift (IS) (Fe) of 0.446 mm/s, which corresponds to $FeCl_3$ [32], after several days the presence of the hydrated phases was noticed, and the IS was 0.260 mm/s.

XRD and MS results were improved with chemical analysis. The quantitative composition of the products is exposed in Table 1, where the different specimen were sorted according to the chlorination temperature and extraction zone. The weight percentage displayed was calculated based on the total content of the metals present, without considering chlorine, water and oxygen.

From Table 1 it can be inferred that the higher the temperature of the zone is the richer the product is in iron; 94.89 wt.% at 175 °C and 96.27 wt.% at 225 °C, while in the coldest areas prevails Al over Fe; 73.34 and 91.93 wt.% of aluminum, respectively. These results prove the XRD characterization for all temperatures of chlorination, showing that at the highest temperature of collection the product is preferably ferric chloride.

Table 1 also exhibits that in a zone over 160 °C condenses only $FeCl_3$ for the chlorination at 200 °C when the voltage supplied to the vertical furnace is about 22 V, whereas, for 26.4 V the product was superimposed with $AlCl_3$, that condenses at a higher temperature.

As regards the theoretical predictions, $FeCl_3$ melts at 304 °C and boils at 319 °C, but has a considerable vapor pressure at 250 °C (6×10^{-3} kPa), that is why the content of iron detected within the $AlCl_3$ at this temperature was higher than the expected values; 10.60 wt.% at 250 °C and 11.50 wt.% at 300 °C. Therefore, the separation of the chlorides decreased as the temperature of the experiment increased, owing to the raising of the ferric chloride volatilization. If the reaction's temperatures continues going up, both chlorides will sublimate together and will deposit all jumbled.

Fig. 4 shows the morphology of the condensed products removed from the top of the vessel after chlorination at 250 °C. The sample had an orange color with green shades and was characterized by XRD as $AlCl_3$.

Table 1
XRD and composition data of the condensed products, after the chlorination of the Fe–Al 50 wt.% mixtures, using the winding

Temperature of chlorination (°C)	Temperature of the extraction zone (°C)	Results of XRD	Composition (wt.%)[a]
175	142–164	$FeCl_3$, $FeCl_3{\cdot}2H_2O$	Al, 5.11; Fe, 94.89
	133	$AlCl_3$	Al, 73.34; Fe, 26.66
200	212–213	$FeCl_3{\cdot}2H_2O$, $FeCl_3{\cdot}5H_2O$	–
	206–218	$AlCl_3$	Al, 18.09; Fe, 81.91
	Room	$AlCl_3$	Al, 92.29; Fe, 8.72
200[b] (22 V)[c]	159–185	$FeCl_3$, $FeCl_3{\cdot}2H_2O$	Al, 24.16; Fe, 75.84
	157–159	$AlCl_3$	Al, 80.13; Fe, 19.87
	Room	$AlCl_3$	Al, 92.17; Fe, 7.83
200[b] (26.4 V)[c]	162–203	$FeCl_3$, $FeCl_3{\cdot}2H_2O$	Al, 19.14; Fe, 80.86
	Room	$AlCl_3$	Al, 91.74; Fe, 8.26
225	190–221	$FeCl_3$, $2FeCl_3{\cdot}7H_2O$	Al, 3.73; Fe, 96.27
	61–146	$AlCl_3$	Al, 91.93; Fe, 8.07
250[b] (26.4 V)[c]	187–235	$FeCl_3$	Al, 7.64; Fe, 92.36
	Room	$AlCl_3$	Al, 89.40; Fe, 10.60
300	270–304	$FeCl_3$, $FeCl_3{\cdot}5H_2O$, $FeCl_3{\cdot}6H_2O$	Al, 8.37; Fe, 91.63
	235–270	$AlCl_3$	Al, 71.22; Fe, 28.78
	220	$AlCl_3$, $AlCl_3{\cdot}6H_2O$	Al, 88.50; Fe, 11.50

[a] Atomic absorption measurement.
[b] Experiments done with the attached vertical furnace.
[c] Voltage supplied to the vertical furnace.

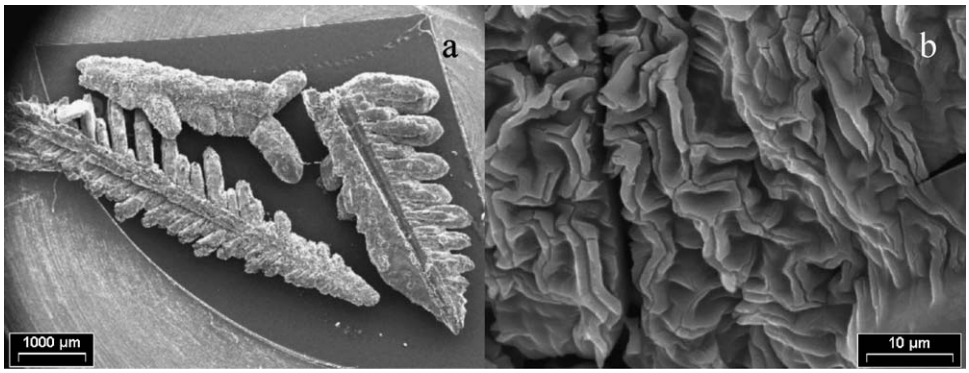

Fig. 4. SEM image of the condensed products removed from the vessel, after chlorination at 250 °C of the mixture Fe–50 wt.% Al: (a) scales formed in the mouth of the vessel, (b) morphology of the surface.

3.3.2. $FeAl_3$

The lowest temperature for the detection of any product was 150 °C and these were extracted near to the reaction zone and from the cold vessel placed at the exit to the gaseous flow.

The samples took out from the vessel exhibit a yellowish color, and were identified as $AlCl_3$, their XRD were similar to those exposed in Fig. 2. There is an effect of preferred orientation on the reflections (0 0 1) and (0 0 2), as seen before on the preceding mixture. In the experiments done at 300 and 200 °C with 12% of power in the vertical furnace, it was detected a slight raising of the background, probably due to the incipient formation of $AlCl_3{\cdot}6H_2O$.

The low temperature product obtained at 200 °C was analysed by Mössbauer spectroscopy, and revealed the presence of Fe^{3+}, with an IS of 0.397 mm/s, whereas, the XRD did not detect $FeCl_3$.

Meanwhile, in the high temperature zones of the reactor, there were dark-green crystals, characterized as $FeCl_3$ like those that can be seen in Fig. 3. However, at 150 °C the samples were constituted by $2FeCl_3{\cdot}7H_2O$ [33].

Like the products of the previous section, ferric chloride showed the preferred orientation on the reflections (0 0 3), for the chlorinations at 175, 200 and 300 °C.

In the lower end of the reactor, adjacent to the $AlCl_3$ placed over the mouth of the vessel, there was a scarce deposit with the aspect of bright green crystals, which became more abundant in proportion to the rise of the temperature, 0.8 cm with at 175 °C, 1.5 cm at 200 °C and 3.5 cm at 250 °C, showing major contamination with iron the more the temperature increases.

Some chemical analysis of the products were performed, as it is shown in Table 2. As the temperature of chlorination raises,

Table 2
XRD and composition data of the condensed products and solid by-products, after the chlorination of the $FeAl_3$ alloy

Temperature of chlorination (°C)	Temperature of the extraction zone (°C)	Results of XRD	Composition (wt.%)[a]
150	Room	$AlCl_3$	Al, 97.41; Fe, 2.59
	138–152	$2FeCl_3{\cdot}7H_2O$	Al, 18.03; Fe, 81.97
	147–152[b]	α-Al_2O_3	Al, 19.25; Fe, 80.75
175	$T > 100$	$AlCl_3$	Al, 93.73; Fe, 6.27
	155–172	$FeCl_3$	Al, 16.77; Fe, 83.23
	168–177[b]	α-Al_2O_3	Al, 95.36; Fe, 4.64
200 (22 V)[c]	Room	$AlCl_3$	–
	156–185	$FeCl_3$	–
	185–196[b]	α-Al_2O_3	–
200 (26.4 V)[c]	Room	$AlCl_3$, $AlCl_3{\cdot}6H_2O$ (traces)	–
	162–203	$FeCl_3$	–
	191–203[b]	α-Al_2O_3	–
250	Room	$AlCl_3$	Al, 90.78; Fe, 9.22
	192–235	$FeCl_3$	Al, 12.92; Fe, 87.08
	247–256[b]	α-Al_2O_3	Al, 94.04; Fe, 5.96
300	Room	$AlCl_3$, $AlCl_3{\cdot}6H_2O$ (traces)	–
	262–298	$FeCl_3$	–
	287–301[b]	α-Al_2O_3	–

[a] Atomic absorption measurement.
[b] The temperature corresponds to the reaction zone.
[c] Voltage supplied to the vertical furnace.

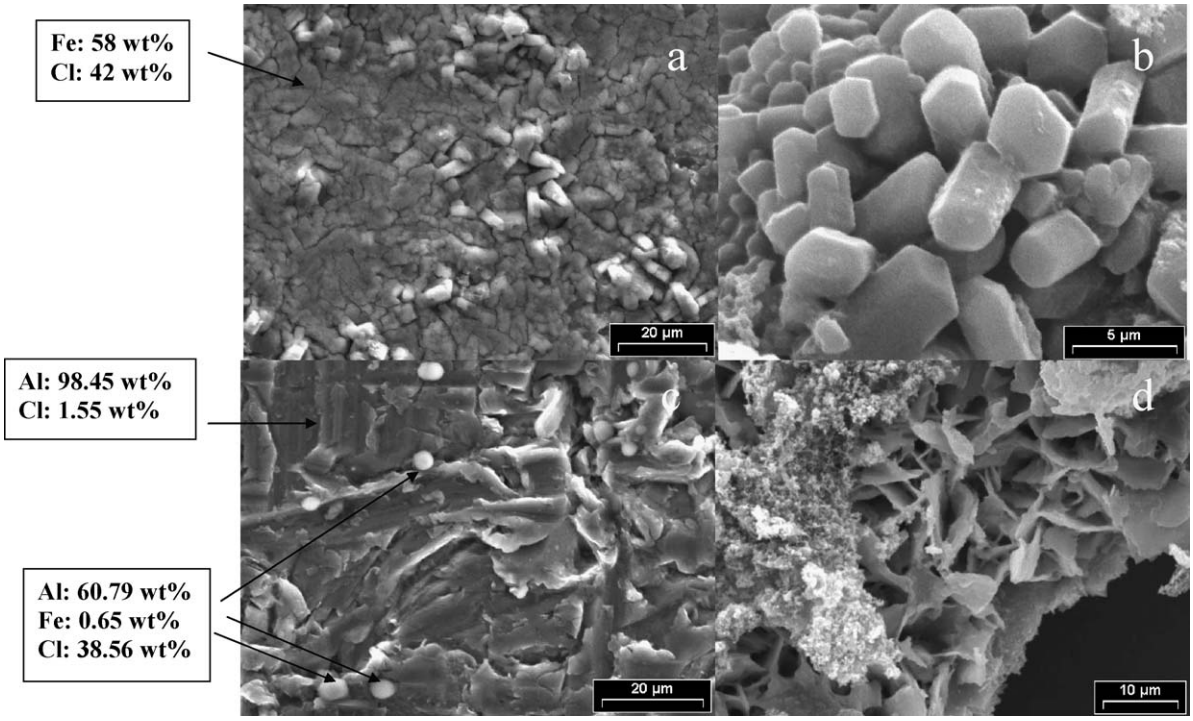

Fig. 5. SEM image of the residues left in the crucible, after chlorination of the mixture Fe–50 wt.% Al, at different temperatures: (a) iron residues at 150 °C and (b) at 275 °C. (c) Aluminum ashes at 150 °C and (d) at 275 °C.

the aluminum chloride extracted enriches from 2.59 to 9.22 wt.% of iron in an increment of 100 °C. The results achieved by XRF confirm the chemical analysis (not shown in the table).

Moreover, the content of iron in $FeCl_3$ also increases with the temperature change, and the quantity of Al decreases from 18.03 to 12.92 wt.%. The last deposits were only constituted by $FeCl_3$, and the high quantity of aluminum should have been detected by XRD, however, the Al measured could be explained if the metal is dissolved in ferric chloride forming a solid solution.

3.4. Analysis of the reaction residues and by-products

The remainder of the reactants and the by-products obtained after chlorination, were left in the glass reaction crucible. They were formed by fragile ashes and small pieces of metal.

3.4.1. Mixture 50 wt.% Fe + Al

The residue was constituted by a dark grey ash of Al and some scraps of Fe. The composition of the remains was fulfilled by EDS at 150 and 300 °C, finding that the ashes of aluminum were composed by 10.59 wt.% of iron at 300 °C, while at 150 °C this element was not detected though a 0.02 wt.% was noticeable by atomic absorption. This result is indicating an increase in the formation of $FeCl_3$ at 300 °C and a portion of this accumulates over the residue.

On the other hand, aluminum was not noticed on the surface of iron chlorinated at 150 °C, but the concentration of chlorine was of 42 and 38 wt.% at 300 °C, due to the initial formation of the chlorides.

Fig. 5a and b shows the morphology exhibited by the remains after chlorination at several temperatures. As the temperature steps up, the crystals of $FeCl_3$ growing over the surface separate from the bulk, revealing their characteristic rhombohedral habit. Concerning to the size, the crystallite have an average length between 3.6 and 10.7 μm.

It can be seen from Fig. 5c that aluminum ashes after chlorination at 150 °C, have fissures all over the surface of the metal because of the attack of the gaseous chlorine and small round grains cover the area, which were constituted by 60.79 wt.% of Al, 0.65 wt.% of Fe and 38.56 wt.% of Cl, determined by EDS.

Fig. 5d corresponds to the aluminum collected after chlorination at 275 °C, with the typical morphology of $AlCl_3$ formed by fragile thin flakes.

3.4.2. $FeAl_3$

From the crucible a greyish powder was collected and characterized by XRD. Samples extracted from the experiments done at 150, 175, 200, 250 and 300 °C revealed being constituted by α-Al_2O_3 [34].

The species α-Al_2O_3, is the most stable phase of the aluminum oxides known as corundum, which belongs to the rhombohedral crystalline system.

According to Table 2, at 175 and 250 °C the samples were mainly constituted by aluminum, while a 5–6 wt.% was iron, tough the XRD technique did not detect any iron compound.

In some samples, orthorhombic aluminum oxychloride was detected by XRD, as well as α-Al_2O_3. The morphology of those residues is exposed in Fig. 6a and b, for an experiment done at 175 °C.

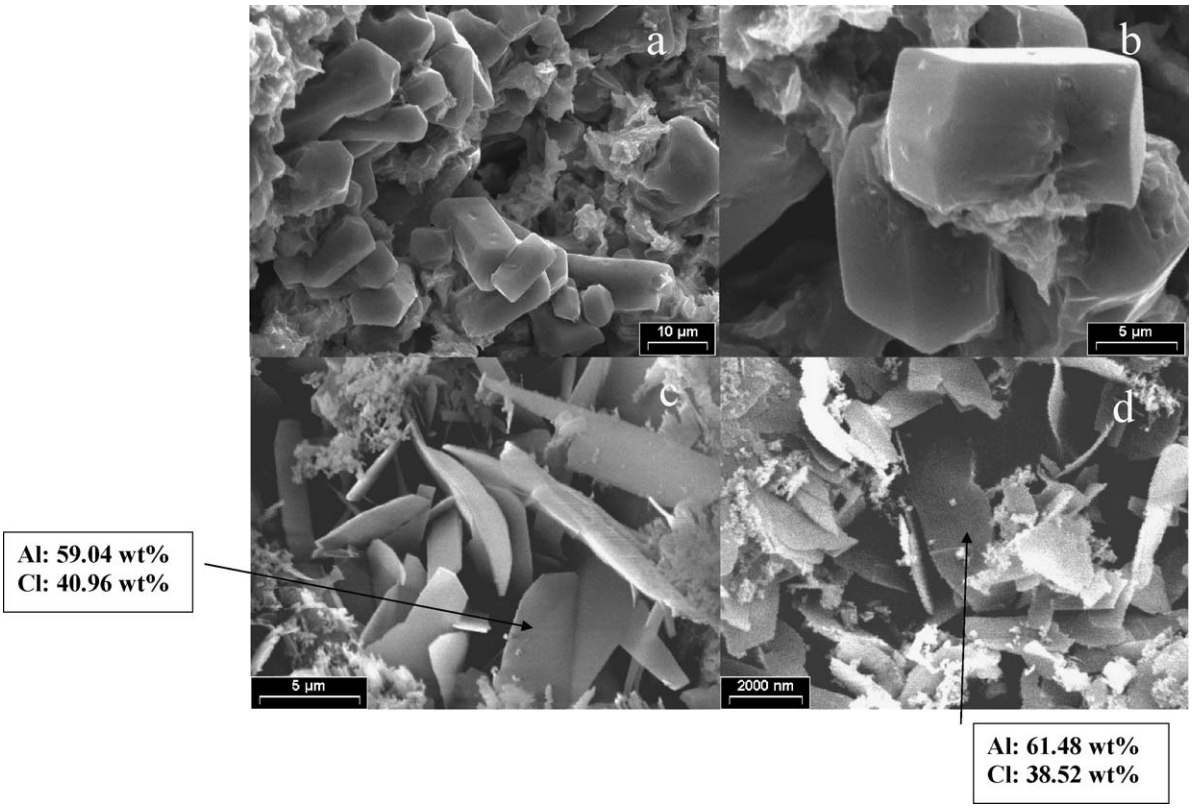

Fig. 6. SEM image of the residues left in the crucible, after chlorination of the alloy $FeAl_3$: (a) and (b) at 175 °C, (c) at 200 °C and (d) at 300 °C.

Because of the fact that AlOCl was not found in most of the samples, a Rietveld simulation [28] of several percentages of mixtures with AlOCl and α-Al_2O_3 was done, in order to find out the lowest detection limit of the oxychloride. From these results can be concluded that below 10 wt.% of AlOCl, the reflection intensities of this compound are so weak that it is possible that in most of the cases the oxychloride may not be detected by XRD.

According to Fig. 6c and d, the appearance of the residues is like very thin flakes, which is typical of the residues that come from the chlorination of the alloy AA6061 [22], that were characterized as $AlCl_3{\cdot}6H_2O$. The last result agree with the composition found by energy dispersive spectroscopy, that is shown in Fig. 6, and though the hexahydrate was not detected in the samples, its most important reflections could be hidden by the raising background in the diffractogram.

3.5. Interpretation of the phenomenology of the separation between Fe and Al in both systems: mixture 50 wt.% Fe + Al and $FeAl_3$

Table 3 compares the composition of $AlCl_3$ and $FeCl_3$ for the two systems under study. For the same temperature, the aluminum chloride obtained from the alloy is richer in Al and is less contaminated with Fe than for the mixture, 96 and 92 wt.% at 200 °C, respectively. As the temperature raises aluminum chloride dissolves more iron, 8 wt.% at 200 °C and 11 wt.% at 250 °C for the mixture, and 4–9 wt.% for the alloy. As the temperature increases, $FeCl_3$ has less Al retained.

The appearance of iron dissolved in the $AlCl_3$ could be a sign of the formation of an adduct constituted by iron, aluminum and chlorine. The formation of the compound happens in gaseous phase, according to the following reactions:

From the pure metals:

$$2Fe + 3Cl_2\,(g) = Fe_2Cl_6\,(g) \quad (a)$$

$$2Al + 3Cl_2\,(g) = Al_2Cl_6\,(g) \quad (b)$$

From the alloy:

$$2FeAl_3 + 12Cl_2\,(g) = Fe_2Cl_6\,(g) + 3Al_2Cl_6\,(g) \quad (c)$$

Table 3
Comparison between the composition of $AlCl_3$ and $FeCl_3$, for the chlorination of the Fe–Al 50 wt.% mixture and the $FeAl_3$ alloy, at 200 and 250 °C

	Temperature (°C)			
	200		250	
	Fe–Al 50 wt.%	$FeAl_3$	Fe–Al 50 wt.%	$FeAl_3$
Aluminum (wt.%)				
$AlCl_3$	92	96	89	91
$FeCl_3$	19	15	8	13
Iron (wt.%)				
$AlCl_3$	8	4	11	9
$FeCl_3$	81	85	92	87

Then the gaseous chlorides interact as it is shown in the chemical equation (d) [35]:

$$Fe_2Cl_6\,(g) + Al_2Cl_6\,(g) = 2FeAlCl_6\,(g) \quad (d)$$

Al_2Cl_6 and Fe_2Cl_6 molecules are stable in the vapor phase and coexist in gaseous mixtures together with $FeAlCl_6$ molecules, the structure of this compound has been inferred from the observed Raman spectrum in vapors [36]. Nalbandian et al. also measured the Raman spectra of the vapor complex in the temperature range 227–627 °C [37].

Other authors did infrared and mass spectrometric studies, finding out that the reaction between ferric chloride and aluminum chloride produces a volatile complex, which transports iron from the reaction zone at temperatures as low as 50 °C. Besides, the complex molecule $FeAlCl_6$ appeared to have a volatility similar to that of $AlCl_3$ [38].

In the range of temperature under study the chlorides are not dissociated, below 440 °C aluminum chloride and iron(III) chloride have the formula Al_2Cl_6 [39] and Fe_2Cl_6 [40], respectively.

Since there are slight differences in the compositions shown in Table 3 for the two systems under study, it can be stated that the formation of $FeAlCl_6$ occurs in the gaseous phase and it is controlled by the vapor pressure of ferric chloride.

In the highest temperature zones ferric chloride dissolves $AlCl_3$, while at the lowest temperature regions aluminum chloride forms solid solutions with $FeCl_3$.

With the purpose of demonstrating the influence of the removal of the complex and the metal chlorides over the concentration of the former at a fixed temperature, additional experiments were done at 175 and 200 °C under different flow rates; 1, 2 and 3.3 l/h of chlorine.

At 175 °C, as the flow rate increases from 1 to 3.3 l/h, the content of iron in aluminum chloride raises from 3.13 to 17.94 wt.%, while the concentration of aluminum in $FeCl_3$ diminishes from 17.61 to 8.71 wt.%.

At 200 °C, Fe in $AlCl_3$ goes up from 11.64 to 29.15 wt.% and aluminum decreases from 10.69 to 7.28 wt.% in $FeCl_3$.

As can be seen from these results, when the flow rate increases the removal of the gaseous species apparently prevails over the formation of $FeAlCl_6$ and consequently less complex is formed. The latter is in agreement with the low aluminum content that was detected in the condensate of the high temperature zone.

For a fixed flow rate, an increment in temperature from 150 to 300 °C, did not show a noticeable change in the iron content present in aluminum chloride, but Al concentration in $FeCl_3$ is lower at higher temperatures, as it is shown in Table 2.

The condensed $FeCl_3$ in the highest temperature zone has a constant complex partial pressure, because the region of deposition has a fixed temperature. Moreover, the concentration of the iron that reaches the low temperature zone as a constituent of the complex, is not expected to change. If a high complex content is desired to be deposited in the cold zone, an increment in the flow rate is needed in order to shift the following equilibrium to the right:

$$FeAlCl_6\ (\text{condensed}) \rightleftarrows FeAlCl_6\ (\text{gaseous}) \quad (e)$$

Table 4
Comparison between Al/Fe ratio in the condensed products ($AlCl_3$ and $FeCl_3$) for the chlorination of the Fe–Al 50 wt.% mixture and the $FeAl_3$ alloy, at different temperatures of reaction

	wt.% Al/wt.% Fe			
	$AlCl_3$		$FeCl_3$	
	Fe–Al 50 wt.%	$FeAl_3$	Fe–Al 50 wt.%	$FeAl_3$
150 °C	–	37.64	–	0.22
175 °C	2.75	14.94	0.05	0.20
200 °C	11.11	25.82	0.24	0.17
225 °C	11.38	–	0.04	–
250 °C	8.44	9.85	0.08	0.15
275 °C	5.69	–	–	–
300 °C	2.47	–	0.09	–

Besides, a raise in the content of Al in $FeCl_3$ from the high temperature zone, shows that reaction (d) is exothermic, and the concentration of the formed complex diminishes with an increment of temperature. When condensating product in the cited zone, equilibrium (e) is displaced to the left in order to keep the complex partial pressure at the condensation temperature.

In Table 4 the data exposed try to show the results in a way that could explain the separation of the elements, iron and aluminum. The second and third columns show the ratio of Al over Fe for $AlCl_3$, demonstrating that as the temperature increases the grade of separation improves for the binary mixture, till 250 °C, when it started to be worst with an increment of temperature. The interpretation is that the bigger is the quotient, less iron is dragged towards the zone where aluminum chloride condenses. On the other hand, in the case of the alloy the tendency is quite different, as temperature goes up the ratio diminishes, and the best value is at 150 °C, however, its separation is still better than that of the mixture, for all the working temperatures.

Fourth and fifth columns corresponds to the ratios for the $FeCl_3$, showing no change with temperature, except for the value for mixture at 200 °C, where the quotient is higher than what it is expected.

Table 5 express the ratio between the percentage of iron present in aluminum chloride condensed at room temperature and the sum of iron percentages in both condensed chlorides ($AlCl_3 + FeCl_3$). The separation factor is showed in a way that as this number increases, it means that the conditions for the separation of the elements get worse. The previous results exhibit that the complete isolation of Fe from Al could not be attained, although at 150 °C is possible to obtain $AlCl_3$ with the least content of iron.

Table 5
Relative percentage of iron, present in the $AlCl_3$ extracted from room temperature's zones, for the chlorination of the Fe–Al 50 wt.% mixture and the $FeAl_3$ alloy

Reagents	Temperature of chlorination (°C)				
	150	200	225	250	300
Fe + Al 50 wt.%	Did not react	9	8	11	12
$FeAl_3$	4	4	–	9	–

4. Conclusions

The starting temperature of the reaction was of 175 °C for the binary mixture of the metals and 150 °C for the alloy.

The reaction advanced with formation of volatile substances, which condense in regions at high and low temperatures and these products resulted to be $FeCl_3$ and $AlCl_3$, respectively. These chemical species exhibited a strong effect of preferred orientation that is more marked in ferric chloride and could be attributed to the typical morphology of thin leaflets that have anisotropic growth and rhombohedral structure, while aluminum chloride forms fragile flakes with pseudohexagonal habit (twinned).

In the condensed phases, Al formed solid solution with $FeCl_3$ and Fe with $AlCl_3$. It is presumed that there is formation of a gaseous complex in vapor phase from the individual chlorides, and in accordance with previous works it is proposed the chemical formula $FeAlCl_6$.

From the results attained it could be deduced that the reaction temperature has little effect on iron content in the $AlCl_3$ that condenses at low temperature. Whereas, the condensing temperature of iron chloride is decisive and this should be the least in order to obtain a minimal partial pressure of the complex.

With the purpose of enhancing the purity of aluminum chloride, we need to reduce the amount of complex formed, by increasing the temperature in the reaction zone, because according to the results found the complex formation is exothermic. An increment in the flow rate favors the volatilization of the complex and this pollutes the condensed $AlCl_3$.

Some separation factors were determined under different experimental conditions for both systems and in none of them the complete separation of the metals was achieved, but at 150 °C it is possible to obtain aluminum chloride with the least iron content.

In all the chlorinations that advanced till complete conversion, α-Al_2O_3 was found in the remains of the alloy in an amount below 3 wt.% of the initial mass. This demonstrates that the oxide scale that is present in the alloy is thicker than that of the pure metals, and this oxide did no react with chlorine at the working temperature.

Acknowledgements

The authors wish to thank the Laboratory of Chemistry from the Company Investigación Aplicada (INVAP, S.C. de Bariloche, Río Negro, Argentina) and the Asentamiento Universitario de Zapala, Univ. Nac. Comahue (Neuquén, Argentina) for the technical help. This work was financially supported by the Agencia Nacional de Promoción Científica y Tecnológica (ANPCYT) with the PICT 10-99-84 and the Consejo Nacional de Investigaciones Científicas y Técnicas (CONICET) with the PIP 2691 project.

References

[1] S.I. Troyanov, Zh. Neorg. Khim. 37 (1992) 266–272.
[2] Kirk-Othmer (Ed.), Encyclopedia of Chemical Technology, vol. 2, Wiley & Sons, New York, 1963, p. 18.
[3] C. Furnas (Ed.), Roger's Industrial Chemistry, vol. 1, Van Nostrand, New York, 1942, p. 462 (Chapter II).
[4] Kirk-Othmer (Ed.), Encyclopedia of Chemical Technology, vol. 2, Wiley & Sons, New York, 1963, p. 36.
[5] H.C. Oersted, Oversigt over det Kongelige Dan. Vid. Sel. For. (1824–1825) 15–16.
[6] R.L. de Beauchamp, Preparation of Anhydrous Aluminum Chloride, Inf. Circ. U.S. Bur. Mines, no. 8412, 1969.
[7] C. Furnas (Ed.), Roger's Industrial Chemistry, vol. 1, Van Nostrand, New York, 1942, p. 460 (Chapter II).
[8] Report from the internet: www.rhodium.ws.
[9] L.S. Belknap, US Patent 3,721,731, Cabot Corporation, Boston, MA, USA (1973).
[10] L. Piccolo, M. Ghirga, B. Calcagno, US Patent 3,812,241, Societa Italiana Resine S. I. R. S. P. A., Milan, Italy (1974).
[11] B.R. Tarr, in: L. Audrieth, et al. (Eds.), Inorganic Synthesis, vol. 3, McGraw-Hill, New York, 1939–1963, p. 191 (Chapter VIII).
[12] J.C. Bailar (Ed.), Comprehensive Inorganic Chemistry, Pergamon Press, Oxford, 1973, p. 67.
[13] H. Schäfer, L. Bayer, Z. Anorg. Allg. Chem. 272 (1953) 265.
[14] I. Kim, W.D. Cho, Mater. Sci. Eng. A 264 (1999) 269–278.
[15] H.C. Ko, A. Landsberg, J.L. Henry, Metall. Trans. B 14 (1983) 301–303.
[16] A.E. Bohé, H.E. Nassini, A.M. Bevilacqua, D.M. Pasquevich, Proceedings of the 21st International Symposium on the Scientific Basis for Nuclear Waste Management XXI, vol. 506, Davos, Switzerland, 1998, pp. 535–542.
[17] A.E. Bohé, A.M. Bevilacqua, H.E. Nassini, D.M. Pasquevich, CD Annais do VII CGEN Trabalho CG33AD, 1998.
[18] A.M. Bevilacqua, A.E. Bohe, H.E. Nassini, D.M. Pasquevich, Global Symposium on Recycling, Waste Treatment and Clean Technology San Sebastián, vol. I, Spain, September 5–9, 1999, pp. 813–825.
[19] A.E. Bohé, F.J. Alvarez, D.M. Pasquevich, Processing Materials for Properties II, San Francisco, California, November 5–8, 2000, pp. 401–406.
[20] F.J. Alvarez, G. De Micco, A.E. Bohé, D.M. Pasquevich, Asociación Argentina de Tecnología Nuclear. XXIX Reunión Anual, Buenos Aires, Argentina, November 19–21, 2002.
[21] F.J. Alvarez, G. De Micco, A.E. Bohé, D.M. Pasquevich, Global Symposium on Recycling Waste Treatment and Clean Technology, vol. III, San Sebastián, Spain, September 26–29, 2004, pp. 2707–2716.
[22] F.J. Alvarez, G. De Micco, A.E. Bohé, D.M. Pasquevich, IAEA, Technical Cooperation Regional Project, RLA/4/018, Final Report, March, 2005.
[23] H.E. Nassini, A.E. Bohé, Proceedings of the Sixth Southern Hemisphere Meeting on Mineral Technology, vol. II, Rio de Janeiro, Brazil, May, 2001, pp. 475–481.
[24] A.E. Bohé, H.E. Nassini, Global Symposium on Recycling, Waste Treatment and Clean Technology, vol. III, San Sebastián, Spain, September 26–29, 2004, pp. 2707–2716.
[25] D.M. Pasquevich, A. Caneiro, Thermochim. Acta 156 (1989) 275–283.
[26] Joint Committee for Powder Diffraction Standards, International Center for Diffraction Data. Powder Diffraction File, 2001. Card number: 77-0819.
[27] Joint Committee for Powder Diffraction Standards, International Center for Diffraction Data. Powder Diffraction File, 2001. Card number: 44-1473.
[28] R.A. Young, A. Sakthivel, T.S. Moss, C.O. Paiva-Santos, J. Appl. Crystallogr. 28 (1995) 366–367.
[29] Joint Committee for Powder Diffraction Standards, International Center for Diffraction Data. Powder Diffraction File, 2001. Card number: 22-0010.
[30] International Union of Crystallography, in: A.J.C. Wilson (Ed.), Structure Reports, Utrecht, IUC, vol. 11, 1947–1948, p. 274.
[31] Joint Committee for Powder Diffraction Standards, International Center for Diffraction Data. Powder Diffraction File, 2001. Card number: 1-1059.
[32] S. DeBenedetti, et al., Phys. Rev. Lett. 6 (2) (1961) 60–62.
[33] Joint Committee for Powder Diffraction Standards, International Center for Diffraction Data. Powder Diffraction File, 2001. Card number: 1-0132.
[34] Joint Committee for Powder Diffraction Standards, International Center for Diffraction Data. Powder Diffraction File, 2001. Card number: 46-1212.
[35] C.F. Shieh, N.W. Gregory, J. Phys. Chem. 79 (8) (1975) 828–833.

[36] Z. Akdeniz, M.P. Tosi, Technical Report IC/99/103, The Abdus Salam International Centre for Theoretical Physics, Miramare, Trieste, 1999.
[37] L. Nalbandian, G.N. Papatheodorou, High Temp. Sci. 28 (1990) 49–65.
[38] R.M. Fowler, S.S. Melford, Inorg. Chem. 15 (2) (1976) 473–474.
[39] J.W. Mellor (Ed.), A Comprehensive Treatise on Inorganic and Theoretical Chemistry, vol. V, Longman, London, 1922–1937, p. 316.
[40] Ullmann's Encyclopedia of Industrial Chemistry, 6th ed., 2002, electronic release.